Dalton Transactions

PAPER

View Article Online
View Journal | View Issue

Cite this: *Dalton Trans.*, 2014, **43**, 13219

Received 29th May 2014,
Accepted 14th July 2014

DOI: 10.1039/c4dt01583e

www.rsc.org/dalton

1,1-Olefin-bridged bis-(2-indenyl) metallocenes of titanium and zirconium†

Jason G. M. Morton,‡[a] Haif Al-Shammari,[b] Yunshan Sun,[a] Jiangtao Zhu[a] and Douglas W. Stephan*[a]

Tetrasubstituted alkenes bearing geminal 2-indenyl substituents – 9-[bis(1*H*-inden-2-yl)methylidene]-9*H*-fluorene (**6**), 2,2′-(2,2-diphenylethene-1,1-diyl)-bis(1*H*-indene) (**7**), and 2,2′-(2-propylpent-1-ene-1,1-diyl)-bis(1*H*-indene) (**8**) have been synthesized and metallated to form a new class of *ansa* titanium and zirconium metallocene complexes containing a single sp^2-hybridized carbon bridge. The synthesis of the tetramethylated bis-indenyl Zr-analog is described. In addition, the 1,1-bis-indenyl ethylene is prepared and the Zr complex is modified by olefin metathesis. X-ray structure analyses reveal strained η^5 sandwich complexes with highly open metal centers. These complexes have proven active in the polymerization of ethylene and its copolymerization with 1-hexene.

Introduction

While heterogeneous Ziegler–Natta titanium and Phillips chromium catalyst systems are currently utilized for the bulk of industrial linear polyethylene production,[1] great attention continues to be directed towards the synthesis and evaluation of homogeneous transition-metal catalysts. Such soluble, single-site species are infinitely variable in their ligand scaffolding, allowing for the designed perturbation of the metal's electronic and structural environment. Soluble catalysts are of particular interest to complement existing heterogeneous high- and low-density polyethylene (HDPE and LDPE) processes through the production of linear low-density polyethylene (LLDPE), where longer α-olefins such as 1-butene, 1-hexene, and 1-octene are incorporated into the polyethylene chain.

Group 4 *ansa*-metallocenes with a single atom bridge continue to be particularly well-studied in this regard,[2–7] though saturation in the academic and patent literature has led many researchers to pursue alternative frameworks.[8–13] Meanwhile, the theoretical[14–17] and structure–activity[2,18–20] analysis of these discreet molecular systems advances our understanding of the polymerization process itself, thereby driving the development of new technology.[21–23]

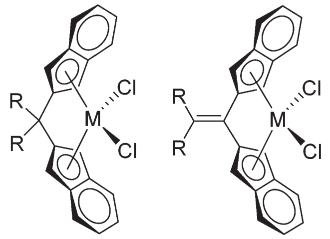

Fig. 1 Metallocene with an sp^2-hybridized bridging carbon.

To our knowledge, there have been no reports of *ansa*-metallocene bridges containing a single, *unsaturated* carbon in the backbone (Fig. 1). We were drawn to such systems in the belief that an sp^2-hybridized carbon would enlarge the angle between the indenyl substituents, and thus provide a more open metallocene than that seen for the corresponding species containing sp^3-carbon center bridges. It is suggested that decreasing the Cp$_{\text{centroid}}$–M–Cp$_{\text{centroid}}$ angle of the metallocene will provide greater α-olefin co-monomer incorporation, possibly due to easier steric access to the cationic metal binding site.[24] Furthermore, unlike traditional substituent variations on the Cp-rings, altering the alkene substituents in such systems will allow for the inductive perturbation of the electronics at the metal center from afar, separating this effect from any steric considerations.

Experimental section

General considerations

Compounds 2-bromoindene (**1**),[25] 9-(dibromomethylene)-fluorene (**3**),[26] (2,2-dibromoethene-1,1-diyl)dibenzene (**4**),[27] 4-(dibromomethylene)heptane (**5**),[28] $(Me_2N)_2ZrCl_2·DME$,[29] and

---

[a] *Department of Chemistry, University of Toronto, 80 St. George St, Toronto, Ontario, Canada, M5S3H6. E-mail: dstephan@chem.utoronto.ca*

[b] *Saudi Basic Industries Corporation, P.O. Box 42503, Riyadh 11551, Saudi Arabia*

† CCDC 1003249–1003258. For crystallographic data in CIF or other electronic format see DOI: 10.1039/c4dt01583e

‡ Current address: SABIC Corporate Research and Innovation Center, P.O. Box 4545-4700, Jeddah-Thuwal, Kingdom of Saudi Arabia, 23955-6900.

$(Me_2N)_2TiCl_2$[30,31] were prepared according to literature precedent. All reactions were carried out and all metallocene complexes were manipulated under an atmosphere of dry N_2 unless otherwise noted. Hexanes, THF, Et_2O, PhMe, and CH_2Cl_2 were dried and deoxygenated using a solvent purification system in the manner of Grubbs,[32] while PhH, PhCl, and 1-hexene were distilled from CaH_2. All solvents were degassed and held over 4 Å molecular sieves prior to use. All other reagents were commercially obtained and used as received. Preparative flash chromatography[33] was performed on Silicycle P60 40–63 μm silica gel. NMR analysis was obtained on Varian Mercury 400, Unity 500, and Brüker Avance III 400 spectrometers. High-temperature GPC analysis for the polymers was performed at Cornell University, Dept. of Chemistry and Chemical Biology with polyethylene calibration. GPC analysis for the ethylene–1-hexene co-polymers was performed at SABIC STC-Riyadh using a Waters Alliance GPC 2000 instrument, with 1,2,4-trichlorobenzene as solvent at 150 °C. Density analysis and differential scanning calorimetry were also performed at SABIC STC-Riyadh. Elemental analysis was performed by the University of Toronto, ANALEST facility, using a PerkinElmer 2400 Series II CHNS Analyzer. In some cases, repeated attempts to acquire satisfactory elemental analyses were unsuccessful.

Synthesis of $(C_9H_7)SnBu_3$ (2). A Schlenk flask was charged with a magnetic stir bar and Mg turnings (5.6 g, 231 mmol, 3.0 eq.) and flame-dried under vacuum. After cooling, the flask was purged to N_2, anhydrous THF was added to just cover the turnings, and stirring was commenced. Two drops of 1,2-dibromoethane were added as initiator, and a heat gun used to briefly reflux the contents, after which the flask was placed in a 25 °C water bath. In a separate flame-dried flask under N_2 atmosphere, 2-bromoindene **1** (15.0 g, 76.9 mmol, 1.0 eq.) was dissolved in 75 mL anhydrous THF. A cannula was then used to transfer this solution onto the activated magnesium turnings over 45 min, resulting in a red, opaque solution. After 1.5 h, GC/MS analysis of an aliquot sample showed consumption of the 2-bromoindene. A separate flame-dried flask under N_2 atmosphere was charged with *n*-Bu_3SnCl (22.9 mL, 84.6 mmol, 1.1 eq.) in 75 mL anhydrous THF and cooled to 0 °C. To this was added, by cannula, the Grignard solution over 20 min., and the reaction flask was brought to ambient temperature for an additional 20 min. The mixture was quenched with chilled, saturated aq. NH_4Cl (50 mL) and the organic phase was separated. The aqueous layer was extracted with Et_2O (50 mL × 3) and the combined organic layers were washed with brine (60 mL), dried over anhydrous $MgSO_4$, filtered, and concentrated to an orange oil. This was pushed through a plug of activated, neutral alumina using hexanes, to provide, after removal of volatiles, the stannane **2** as a yellow oil (27.7 g, ~95 weight% purity by NMR) which was used without further purification. (The product is unstable to normal SiO_2 chromatography, while an attempt at vacuum distillation was unsuccessful). ^{1}H-NMR (300 MHz, $CDCl_3$) δ 7.51 (d, J = 7.3 Hz, 1H, H_{arom}), 7.42 (d, J = 7.4 Hz, 1H, H_{arom}), 7.29 (t, J = 7.3 Hz, 1H, H_{arom}), 7.17 (td, J = 7.4, 1.1 Hz, 1H, H_{arom}), 7.09 (s, 1H, C*H*CCH_2), 3.52 (d, J = 1.8 Hz, 2H, $CHCCH_2$), 1.79–1.49 (m, 6H, $CH_2CH_2CH_2CH_3$), 1.47–1.29 (m, 6H, $CH_2CH_2CH_2CH_3$), 1.11–1.12 (m, 6H, $CH_2CH_2CH_2CH_3$), 0.94 (t, J = 7.3 Hz, 9H, $CH_2CH_2CH_2CH_3$). ^{13}C-NMR (75 MHz, $CDCl_3$) δ 149.92, 147.00, 145.56, 141.81 (J_{C-Sn} = 16.4 Hz), 126.06, 123.92, 123.21, 119.97, 45.85 (J_{C-Sn} = 20.8, 20.0 Hz), 29.23 (J_{C-Sn} = 10.5 Hz), 27.36 (J_{C-Sn} = 28.5, 27.2 Hz), 13.69, 9.69 (J_{C-Sn} = 173, 166 Hz).

Synthesis of $(C_{12}H_8)C{=}C(C_9H_7)_2$ (6). In a flame-dried Schlenk flask under N_2 atmosphere were combined 9-(dibromomethylene)fluorene (**3**) (2.0 g, 5.95 mmol, 1.0 eq.) and tributyl(1*H*-inden-2-yl)stannane (**2**) (6.03 g, 14.9 mmol, 2.5 eq.). Magnetic stirring commenced, and the contents were degassed under vacuum for 15 min. The flask was purged with N_2, then charged with 30 mL anhydrous, degassed toluene. $Pd_2(dba)_3$ (272 mg, 0.30 mmol, 0.05 eq.) and *t*-Bu_3P (240 mg, 1.2 mmol, 0.2 eq.) were combined in 3 mL anhydrous, degassed toluene and syringed into the reaction mixture. This was followed by three freeze–pump–thaw cycles, then reintroduction of N_2 atmosphere. The reaction mixture was then heated at 100 °C for 14 h. After this time, the solution was allowed to cool to ambient temperature, and KF (3.46 g, 59.5 mmol, 10 eq.) and 30 mL H_2O were added and the resultant biphasic mixture was stirred vigorously for 1 h. The crude product was then filtered through Celite, with EtOAc (100 mL) as additional elutant. After aqueous separation with brine (30 mL), the organic layer was dried with $MgSO_4$ and concentrated by rotary evaporation onto 2 g of silica. Column chromatography (5 → 10 → 20 → 30% PhMe–hexanes; the product can be seen as a red band) provided the desired **6** (2.05 g, 85% yield) as a bright red solid. ^{1}H-NMR (200 MHz, $CDCl_3$) δ 7.73 (d, J = 7.5 Hz, 2H, H_{arom}), 7.46 (dd, J = 7.5, 5.2 Hz, 6H, H_{arom}), 7.40–7.19 (m, 6H, H_{arom}), 7.13–6.98 (m, 4H), 3.72 (s, 4H, $CHCCH_2$). ^{13}C-NMR (101 MHz, $CDCl_3$) δ 148.45, 144.73, 143.99, 140.25, 138.49, 137.06, 134.96, 133.40, 127.67, 126.80, 125.35, 124.80, 123.96, 121.70, 119.49, 40.95. Analysis calc'd for $C_{32}H_{22}$ (406.52 g mol^{-1}): C, 94.55; H, 5.45; found: C, 94.08; H, 5.83.

Synthesis of $Ph_2C{=}C(C_9H_7)_2$ (7). In the same manner as **6**, **7** was synthesized from (2,2-dibromoethene-1,1-diyl)dibenzene **4** (6.55 g, 19.4 mmol, 1.0 eq.), tributyl(1*H*-inden-2-yl)stannane **2** (19.65 g, 48.5 mmol, 2.5 eq.), $Pd_2(dba)_3$ (890 mg, 0.97 mmol, 0.05 eq.), *t*-Bu_3P (790 mg, 3.9 mmol, 0.2 eq.) and KF (11.3 g, 19.5 mmol, 10 eq.) in dry toluene (100 mL). Column chromatography (5 → 10 → 20 → 30 → 40% PhMe–hexanes; the product can be seen as a yellow band) provided **7** (5.17 g, 65% yield) as a bright yellow solid. ^{1}H-NMR (400 MHz, $CDCl_3$) δ 7.43–7.27 (m, 16H, H_{arom}), 7.24 (td, J = 7.2, 1.5 Hz, 2H, H_{arom}), 6.84 (s, 2H, C*H*CCH_2), 3.34 (s, 4H, $CHCCH_2$). ^{13}C-NMR (101 MHz, $CDCl_3$) δ 150.00, 144.61, 143.86, 143.77, 141.27, 134.11, 133.06, 130.45, 128.06, 126.98, 126.23, 124.54, 123.36, 120.86, 41.25. Analysis calc'd for $C_{32}H_{24}$ (408.53 g mol^{-1}): C, 94.08; H, 5.92; found: C, 93.61; H, 6.21.

Synthesis of *n*-$Pr_2C{=}C(C_9H_7)_2$ (8). In the same manner as **6** except that 4-(dibromomethylene)heptane **5** was added once after stannane reagent was degassed, **8** was synthesized from **5** (5.26 g, 19.5 mmol, 1.0 eq.), tributyl(1*H*-inden-2-yl)stannane **2**

(19.8 g, 48.9 mmol, 2.5 eq.), $Pd_2(dba)_3$ (890 mg, 0.97 mmol, 0.05 eq.), *t*-Bu_3P (790 mg, 3.9 mmol, 0.2 eq.) and KF (11.3 g, 19.5 mmol, 10 eq.) in dry toluene (100 mL). Column chromatography (5% PhMe–hexanes) provided **8** (4.8 g, 72% yield) as a slightly yellow, viscous oil. ^{1}H-NMR (400 MHz, $CDCl_3$) δ 7.30 (d, J = 7.4 Hz, 2H, H_{arom}), 7.23 (dd, J = 14.1, 7.3 Hz, 4H, H_{arom}), 7.11 (td, J = 7.4, 1.1 Hz, 2H, H_{arom}), 6.64 (s, 2H, C*H*CCH$_2$), 3.26 (s, 4H, CHCC*H*$_2$), 2.36–2.04 (m, 4H, C*H*$_2$CH$_2$CH$_3$), 1.56–1.36 (m, 4H, CH$_2$C*H*$_2$CH$_3$), 0.84 (t, J = 7.3 Hz, 6H, CH$_2$CH$_2$C*H*$_3$). ^{13}C-NMR (100 MHz, $CDCl_3$) δ 148.78, 145.60, 143.65, 141.13, 130.83, 129.89, 126.80, 124.66, 123.85, 121.04, 42.51, 34.94, 22.53, 14.31. Analysis calc'd for $C_{26}H_{28}$ (340.50 g mol^{-1}): C, 91.71; H, 8.29; found C, 91.30; H 8.40.

Synthesis of $(C_{12}H_8)C{=}C(C_9H_6)_2TiCl_2$ (9a). In the glovebox, under N_2 atmosphere, a vial was charged with 9-(di(1*H*-inden-2-yl)methylene)fluorene (**6**) (73 mg, 0.180 mmol, 1.0 eq.) and 3.6 mL THF. The mixture was stirred magnetically and cooled to −35 °C, after which time solid NaHMDS (69 mg, 0.377 mmol, 2.1 eq.) was added in one portion. The reaction was allowed to warm slowly to ambient temperature and stirred for a total time of 5 h. The homogeneous solution was then cooled back to −35 °C and solid $(Me_2N)_2TiCl_2$ (39.1 mg, 0.189 mmol, 1.05 eq.) was added. The reaction mixture was allowed to warm slowly to ambient temperature and stirred overnight. After this time, the THF was removed *in vacuo*. The residue was filtered through Celite with PhH (6 mL), concentrated, and washed with pentanes (2 mL × 5) to remove trace remaining $(Me_2N)_2TiCl_2$. The resultant dark purple residue was dissolved in 1.5 mL CH_2Cl_2, after which Me_3SiCl (0.06 mL, 0.46 mmol, 3.0 eq.) was added. The reaction mixture was stirred magnetically for 12 h, then the volatiles were removed *in vacuo*. The purple residue was added to a small pipet packed with Celite. It was washed with PhH, which was then discarded. The remaining solids were then filtered through using PhCl, which after concentration and precipitation from hexanes provided **9a** (38 mg, 48% yield) as a purple solid. Crystals suitable for X-ray diffraction could be grown by vial-in-vial solvent diffusion of a concentrated solution of **9a** in PhCl with hexanes. ^{1}H-NMR (500 MHz, C_6D_5Br) δ 7.84 (d, J = 7.7 Hz, 2H, H_{arom}), 7.81 (d, J = 7.6 Hz, 2H, H_{arom}), 7.73 (dd, J = 6.5, 3.1 Hz, 4H, H_{arom}), 7.47 (dt, J = 7.6, 1.1 Hz, 2H, H_{arom}), 7.30 (dd, J = 6.4, 3.1 Hz, 4H, H_{arom}), 7.17 (dt, J = 7.6, 1.1 Hz, 2H, H_{arom}), 6.24 (s, 4H, C*H*CC*H*). ^{13}C-NMR (partial, by gHMBC; C_6D_5Br) δ 141.5, 137.4, 133.9, 130.0, 128.4, 127.9, 126.3, 125.3, 120.7, 113.1, 109.4. Analysis calc'd for $C_{32}H_{20}Cl_2Ti{\cdot}C_6H_5Cl$ (634.05 g mol^{-1}): C, 71.78; H, 3.96; found: C, 71.92; H, 4.39.

Synthesis of $Ph_2C{=}C(C_9H_6)_2TiCl_2$ (10a). In the same manner as **9a** except that a different purification method was employed, **10a** was synthesized from 2,2′-(2,2-diphenylethene-1,1-diyl)bis(1*H*-indene) **7** (295 mg, 0.72 mmol, 1.0 eq.), NaHMDS (278 mg, 1.52 mmol, 2.2 eq.) and $(Me_2N)_2TiCl_2$ (180 mg, 0.76 mmol, 1.05 eq.) in THF (6 mL), and Me_3SiCl (0.6 mL, 4.73 mmol, 6.5 eq.) in CH_2Cl_2 (6 mL). The mixture of **10a** in CH_2Cl_2 was concentrated and the dark residue was washed with a 3 : 1 pentane–Et_2O solution (1 mL × 2). The remaining solids were then filtered through Celite using CH_2Cl_2 (5 mL), which after concentration provided **10a** (210 mg, 56% yield) as a purple solid. Crystals suitable for X-ray diffraction could be grown by layering hexanes over a concentrated solution of **10a** in CH_2Cl_2. ^{1}H-NMR (400 MHz, CD_2Cl_2) δ 7.58–7.53 (m, 4H, H_{arom}), 7.49 (dd, J = 6.5, 3.1 Hz, 4H, H_{arom}), 7.40–7.26 (m, 10H, H_{arom}), 6.18 (s, 4H, C*H*CC*H*). ^{13}C-NMR (101 MHz, CD_2Cl_2) δ 144.60, 139.39, 133.72, 130.41, 128.92, 128.87, 128.78, 128.11, 127.16, 126.07, 114.83, 110.89. Analysis calcd for $C_{32}H_{22}Cl_2Ti{\cdot}CH_2Cl_2$ (612.24): C, 64.95; H, 3.96; found: C, 64.43; H, 3.84.

Synthesis of *n*-$Pr_2C{=}C(C_9H_6)_2TiCl_2$ (11a). In the same manner as **9a** except that a different purification method was employed, **11a** was synthesized from 2,2′-(2-propylpent-1-ene-1,1-diyl)bis(1*H*-indene) (**8**) (206 mg, 0.605 mmol, 1.0 eq.), NaHMDS (233 mg, 1.27 mmol, 2.1 eq.) and $(Me_2N)_2TiCl_2$ (131 mg, 0.635 mmol, 1.05 eq.) in THF (6 mL), and Me_3SiCl (0.45 mL, 3.6 mmol, 6.0 eq.) in CH_2Cl_2 (5 mL). The dark residue was added to a small pipet packed with Celite and filtered through using CH_2Cl_2. Removal of solvent *in vacuo*, then washing/decanting the resultant purple solid with pentanes (5 mL × 3) provided **11a** (130 mg, 47% yield) as a purple solid. Crystals suitable for X-ray diffraction were grown by vial-in-vial solvent diffusion of a concentrated solution of **11a** in CH_2Cl_2 with hexanes. ^{1}H-NMR (400 MHz, C_6D_6) δ 7.47 (dd, J = 6.4, 2.9 Hz, 4H, H_{arom}), 7.01 (dd, J = 6.4, 2.9 Hz, 4H, H_{arom}), 5.65 (s, 4H, C*H*CC*H*), 2.19 (t, J = 7.4 Hz, 4H, C*H*$_2$CH$_2$CH$_3$), 1.59–1.34 (m, 4H, CH$_2$C*H*$_2$CH$_3$), 0.86 (t, J = 7.3 Hz, 6H, CH$_2$CH$_2$C*H*$_3$). ^{13}C-NMR (101 MHz, C_6D_6) δ 142.37, 133.49, 127.81, 125.71, 125.34, 114.60, 109.56, 33.16, 21.40, 13.99. Analysis calcd for $C_{26}H_{26}Cl_2Ti$ (457.26): HC, 68.29; H, 5.73; found: C, 68.15; H, 5.88.

Synthesis of $(C_{12}H_8)C{=}C(C_9H_6)_2ZrCl_2$ (9b). In the same manner as **9a** except that a different purification method was employed, **9b** was synthesized from 9-(di(1*H*-inden-2-yl)-methylene)fluorene (**6**) (92 mg, 0.226 mmol, 1.0 eq.), NaHMDS (91.3 mg, 0.498 mmol, 2.2 eq.) and $(Me_2N)_2ZrCl_2{\cdot}DME$ (81 mg, 0.237 mmol, 1.05 eq.) in THF (4 mL), and Me_3SiCl (0.18 mL, 1.8 mmol, 6.0 eq.) in CH_2Cl_2 (5 mL). The residue washed with Et_2O (2 mL × 2), then hexanes (6 mL × 3) to provide, after removal of trace solvent *in vacuo*, the desired **9b** (114 mg, 89% yield) as an orange, highly insoluble solid. Crystals suitable for X-ray diffraction were grown by slow precipitation of a PhMe–PhH solution. ^{1}H-NMR (400 MHz, C_6D_6) δ 7.60 (d, J = 7.7 Hz, 2H, H_{arom}), 7.53 (d, J = 7.6 Hz, 2H, H_{arom}) 7.50 (dd, J = 6.5, 3.1 Hz, 4H, H_{arom}), 7.16 (dt, J = 1.0, 7.6 Hz, 2H, H_{arom}), 6.97 (dd, J = 3.1, 6.5 Hz, 4H, H_{arom}), 6.88 (dt, J = 1.1, 7.6 Hz, 2H, H_{arom}), 5.68 (s, 4H, C*H*CC*H*). ^{13}C-NMR (100 MHz, C_6D_6) δ 141.3, 137.4, 129.5, 129.2, 128.5, 127.6, 127.1, 126.9, 125.3, 125.0, 120.3, 116.6, 101.7. Analysis calc'd for $C_{32}H_{22}Cl_2Zr{\cdot}C_6H_5Cl$ (681.20 g mol^{-1}): C, 67.20; H, 3.71; found: C, 66.90; H, 4.07.

Synthesis of $Ph_2C{=}C(C_9H_6)_2ZrCl_2$ (10b). In the same manner as **9a** except that a different purification method was employed, **10b** was synthesized from 2,2′-(2,2-diphenylethene-1,1-diyl)bis(1*H*-indene) **7** (2 g, 4.90 mmol, 1.0 eq.), NaHMDS (1.98 g, 10.8 mmol, 2.2 eq.) and $(Me_2N)_2ZrCl_2{\cdot}DME$ (1.91 g, 5.16 mmol, 1.05 eq.) in THF (50 mL), and Me_3SiCl (2.2 mL, 17.3 mmol, 3.5 eq.) in CH_2Cl_2 (25 mL). The mixture of **10b** in CH_2Cl_2 was concentrated and the resulting residue was dissolved in CH_2Cl_2 (5 mL), after which time slow addition of hexanes causes precipitation of the desired complex. The supernatant was decanted, and the procedure repeated, to give **10b** (2.1 g, 71%) as a yellow powder. Crystals suitable for X-ray diffraction were grown by layering a concentrated solution of **10b** in CH_2Cl_2 with pentane. ^1H-NMR (400 MHz, C_6D_6) δ 7.57–7.47 (m, 4H, H_{arom}), 7.39 (dd, J = 6.5, 3.1 Hz, 4H, H_{arom}), 7.10–6.93 (m, 6H, H_{arom}), 6.90 (dd, J = 6.5, 3.1 Hz, 4H, H_{arom}), 5.62 (s, 4H, C*H*CC*H*). ^{13}C-NMR (100 MHz, C_6D_6) δ 144.39, 139.64, 130.27, 128.67, 128.54, 128.51, 128.26 (found by gHMBC) 126.57, 124.86, 117.73, 102.64. Analysis calcd for $C_{32}H_{22}Cl_2{\cdot}C_6H_5Cl$ (681.20): C, 67.00; H, 4.00; found: C, 67.19; H, 4.38.

Synthesis of *n*-$Pr_2C{=}C(C_9H_6)_2ZrCl_2$ (11b). In the same manner as **9a** except that a different purification method was employed, **11b** was synthesized from 2,2′-(2-propylpent-1-ene-1,1-diyl)bis(1*H*-indene) **8** (130 mg, 0.382 mmol, 1.0 eq.), NaHMDS (147 mg, 0.802 mmol, 2.1 eq.) and $(Me_2N)_2ZrCl_2{\cdot}DME$ (137 mg, 0.401 mmol, 1.05 eq.) in THF (8 mL), and Me_3SiCl (0.14 mL, 1.1 mmol, 3.0 eq.) in CH_2Cl_2 (4 mL). The mixture of **11b** in CH_2Cl_2 was concentrated and the residue was washed with a 5 : 1 pentane–Et_2O solution (1 mL × 2). The remaining solids were then filtered through Celite using PhH (5 mL), which after concentration provided **11b** (155 mg, 81% yield) as a yellow solid. ^1H-NMR (400 MHz, C_6D_6) δ 7.47 (dd, J = 6.5, 3.1 Hz, 4H, H_{arom}), 6.97 (dd, J = 6.5, 3.1 Hz, 4H, H_{arom}), 5.57 (s, 4H, C*H*CC*H*), 2.24–2.15 (m, 4H, $CH_2CH_2CH_3$), 1.59–1.35 (m, 4H, $CH_2CH_2CH_3$), 0.86 (t, J = 7.4 Hz, 6H, $CH_2CH_2CH_3$). ^{13}C-NMR (101 MHz, C_6D_6) δ 143.01, 129.08, 126.53, 125.70, 124.88, 118.16, 102.54, 33.09, 21.47, 13.98. Analysis calcd for $C_{26}H_{26}Cl_2Zr$ (500.61): C, 62.38; H, 5.23; found: C, 62.23; H, 5.41.

Synthesis of $(C_{12}H_8)C{=}C(C_9H_5Me_2)_2$ (12). To a solution of **6** (1.3 g, 3.2 mmol, 1.0 eq.) in THF (20 mL) was added $NaN(SiMe_3)_2$ (1.2 g, 6.7 mmol, 2.1 eq.) in one portion at −35 °C. The resulting purple solution was allowed to warm slowly to ambient temperature and stirred for 3 h. Then the reaction mixture was cooled in an ice bath and MeI (1.9 g, 13.4 mmol, 4.2 eq.) was added. After stirred overnight, the reaction was quenched by saturated NH_4Cl solution (10 mL) and extracted by ether (30 mL × 2). The organic layer was dried over $MgSO_4$, filtered and concentrated to give the crude dimethylated intermediate (1.1 g). The dimethylated intermediate was dissolved in THF (30 mL) and cooled to −35 °C. $LiN(SiMe_3)_2$ (876 mg, 5.25 mmol, 2.1 eq.) was added in one portion. The resulting solution was stirred at ambient temperature for 3 h. Then the reaction mixture was cooled in an ice bath and MeI (1.7 g, 12.0 mmol, 4.8 eq.) was added. After stirred overnight, the reaction was quenched by saturated NH_4Cl solution (10 mL) and extracted by ether (30 mL × 2). The organic layer was dried over $MgSO_4$, filtered and concentrated. The residue was recrystallized by DCM and MeOH to give the product (**12**) (815 mg, 55% yield). ^1H-NMR (400 MHz, $CDCl_3$) δ 7.78 (ddt, J = 13.0, 8.0, 0.9 Hz, 4H, H_{arom}), 7.48–7.39 (m, 8H, H_{arom}), 7.35–7.31 (m, 4H, H_{arom}), 7.14–7.07 (m, 2H, H_{arom}), 3.58 (qd, J = 7.5, 3.8 Hz, 2H, C*H*CH_3). 2.10 (d, J = 2.0 Hz, 6H, CCH_3), 1.40 (d, J = 7.6 Hz, 6H, $CHCH_3$). ^{13}C-NMR (100 MHz, $CDCl_3$) δ 148.94, 147.17, 145.04, 140.07, 138.46, 137.56, 137.12, 134.51, 127.60, 127.18, 126.81, 125.71, 123.94, 122.65, 119.98, 119.23, 46.85, 15.23, 12.15. HRMS (*m*/*z*) calcd for $C_{36}H_{31}[M + H^+]$ 463.24258, found 463.24230.

Synthesis of $(C_{12}H_8)C{=}C(C_9H_4Me_2)_2$ (13). Under N_2 atmosphere, a vial was charged with **12** (185 mg, 0.4 mmol, 1.0 eq.) and THF (10 mL). The mixture was stirred magnetically and cooled to −35 °C, then solid $NaN(SiMe_3)_2$ (154 mg, 0.84 mmol, 2.1 eq.) was added in one portion; the reaction mixture immediately went to a deep purple color. The reaction was allowed to warm slowly to ambient temperature and stirred for a total time of 5 h. The homogeneous solution was then cooled back to −35 °C and solid $(Me_2N)_2TiCl_2$ (86 mg, 0.42 mmol, 1.05 eq.) was added in one portion. The reaction mixture was allowed to warm slowly to ambient temperature and stirred overnight. After this time, the THF was removed *in vacuo*. Hexane (16 mL) washed the residue solid and the filtrate was vacuumed to give the product (**13**) (120 mg, 65% yield) as a purple solid. ^1H-NMR (400 MHz, CD_2Cl_2) δ 7.86 (d, J = 6.5 Hz, 2H, H_{arom}), 7.70 (d, J = 7.1 Hz, 2H, H_{arom}), 7.68–7.62 (m, 2H, H_{arom}), 7.52–7.47 (m, 2H, H_{arom}), 7.44–7.38 (m, 4H, H_{arom}), 7.37–7.27 (m, 4H, H_{arom}), 1.99 (s, 6H, $C{=}CCH_3$), 0.79 (s, 6H, CCH_3). ^{13}C-NMR (100 MHz, CD_2Cl_2) δ 160.20, 150.15, 148.01, 139.93, 139.35, 139.21, 130.96, 130.68, 127.73, 127.02, 127.00, 126.78, 124.78, 123.55, 121.34, 119.92, 62.97, 18.23, 15.35. HRMS (*m*/*z*) calcd for $C_{36}H_{29}$ $[M + H^+]$ 461.22693, found 461.22532.

Synthesis of $(C_{12}H_8)C{=}C(C_9H_4Me_2)_2ZrCl_2$ (14). In the glovebox, under N_2 atmosphere, a vial was charged with **12** (140 mg, 0.3 mmol, 1.0 eq.) and THF (10 mL). The mixture was stirred magnetically and cooled to −35 °C, then solid NaHMDS (122 mg, 0.63 mmol, 2.1 eq.) was added in one portion; the reaction mixture immediately went to a deep purple color. The reaction was allowed to warm slowly to ambient temperature and stirred for a total time of 5 h. The homogeneous solution was then cooled back to −35 °C and solid $(Me_2N)_2ZrCl_2{\cdot}DME$ (107 mg, 0.31 mmol, 1.05 eq.) was added. The reaction mixture was allowed to warm slowly to ambient temperature and stirred overnight. After this time, the THF was removed *in vacuo*. The brown residue was filtered through Celite with CH_2Cl_2 (10 mL) and concentrated. The resulting solid was dissolved in CH_2Cl_2 (10 mL), after which Me_3SiCl (194 mg, 1.8 mmol, 3.0 eq.) was added. The reaction mixture was stirred magnetically at ambient temperature for 12 h, during which time red precipitates crash out. The volatiles were removed *in vacuo*, and the residue washed with hexanes (15 mL). The supernatant was decanted off, and the residue washed with further CH_2Cl_2 (6 mL × 3) to provide, after removal of trace solvent *in vacuo*, the desired **14** (112 mg, 60% yield) as a yellow solid. Crystals suitable for X-ray diffraction were grown by slow precipitation of a CH_2Cl_2–hexane solution. ^1H-NMR (400 MHz, CD_2Cl_2) δ 7.83 (dt, J = 7.6, 0.9 Hz, 2H, H_{arom}), 7.58–7.49 (m, 6H, H_{arom}), 7.43 (td, J = 7.5, 1.1 Hz, 2H, H_{arom}), 7.37–7.27

(m, 4H, H_{arom}), 7.16 (td, J = 7.6, 1.1 Hz, 2H, H_{arom}), 2.46 (s, 12H, CCH_3). ^{13}C-NMR (100 MHz, CD_2Cl_2) δ 141.00, 140.31, 137.11, 129.82, 129.30, 127.78, 125.63, 124.20, 124.13, 123.53, 120.00, 114.02, 111.03, 14.72.

Synthesis of (HO)CMe(C_9H_7)$_2$ (15). Under N_2 atmosphere, a flask was charged with the indenyl Grignard solution, prepared from 2-bromoindene (1.56 g, 8 mmol, 1.0 eq.) and Mg turnings (0.576 g, 24 mmol, 3.0 eq.) in THF (16 mL). To this flask was added acetyl chloride (234 mg, 3.0 mmol) dropwise by syringe. The resulting mixture was stirred for another 1 h at room temperature. Then workup by NH_4Cl saturated solution (10 mL) and extracted by ether (50 mL). The organic layers was dried over $MgSO_4$, filtered and concentrated. The residue was further purified by silica gel column by Hexane to give the product (**15**) (207 mg, 25% yield). ^{1}H-NMR (400 MHz, $CDCl_3$) δ 7.39–7.31 (m, 4H, H_{arom}), 7.28–7.19 (m, 2H, H_{arom}), 7.14 (td, J = 7.4, 1.2 Hz, 2H, H_{arom}), 6.79 (dt, J = 1.6, 0.8 Hz, 2H, $CHCCH_2$), 3.51–3.33 (m, 4H, $CHCCH_2$), 1.85 (s, 3H). ^{13}C-NMR (100 MHz, $CDCl_3$) δ 154.53, 144.52, 143.39, 126.57, 124.76, 123.83, 121.11, 73.65, 38.33, 28.93. HRMS (m/z) calcd for $C_{20}H_{17}[M - OH]^+$ 257.13303, found 257.13365.

Synthesis of C_3HMe(C_9H_7)$_4$ (16). To a solution of compound (**15**) (137 mg, 0.5 mmol, 1.0 eq.) in DCM (3 mL) was added some crystals of *p*-toluenesulfonic acid (10 mg, 0.05 mmol, 0.1 eq.). The resulting solution was stirred at 40 °C for 1 h. The solution was then washed with brine (10 mL) and extracted with DCM (10 mL × 2). The organic layers were dried over Na_2SO_4, filtered and concentrated. The residue was further purified by silica gel column (hexane–DCM = 2 : 1) to give the product (**16**) (68 mg, 50% yield). ^{1}H-NMR (400 MHz, $CDCl_3$) δ 7.67 (d, J = 7.1 Hz, 1H), 7.52–6.88 (m, 16H), 6.40 (d, J = 3.9 Hz, 1H), 4.30–3.12 (m, 11H), 2.07–1.94 (m, 3H). ^{13}C-NMR (100 MHz, $CDCl_3$) δ 145.89, 145.70, 145.53, 144.43, 143.94, 143.90, 143.53, 142.24, 141.70, 141.66, 138.56, 129.51, 127.12, 127.08, 127.00, 126.87, 126.68, 125.74, 125.71, 125.70, 125.56, 125.15, 124.87, 124.78, 124.54, 124.40, 124.05, 123.48, 122.17, 121.01, 57.53, 54.40, 53.77, 51.88, 47.25, 39.94, 39.47, 39.24, 35.77, 18.04. HRMS (m/z) calcd for $C_{40}H_{33}$ [M + H$^+$] 513.25283, found 513.25531.

Synthesis of (C_9H_7)C≡CSiMe$_3$ (17). To a Schlenk flask was charged with 2-bromoindene (6 g, 30.8 mmol, 1.0 eq.), CuI (0.59 g, 3.1 mmol, 0.1 eq.), THF (80 mL) and triethylamine (20 mL), and it was freeze–pump–thaw three times. Trimethylsilylacetylene (5.2 mL, 37.5 mmol, 1.2 eq.) and $PdCl_2(PPh_3)_2$ (0.6 g, 0.9 mmol, 0.03 eq.) was then added under N_2 atmosphere. The resulting mixture was stirred at room temperature overnight, and TLC (hexane) showed the reaction was done. The mixture was filtered and the filter cake was washed with hexane (20 mL × 3). The combined filtrates was washed with brine (50 mL × 1), dried over $MgSO_4$, filtered and evaporated *in vacuo*. The residue was purified by silica gel column (0 → 5% CH_2Cl_2–hexane) to give **2** (6 g, 92% yield) as a yellow solid. ^{1}H-NMR (400 MHz, $CDCl_3$) δ 7.40 (d, J = 7.2 Hz, 1H, H_{arom}), 7.37 (d, J = 7.4 Hz, 1H, H_{arom}), 7.28 (t, J = 6.8 Hz, 1H, H_{arom}), 7.23 (t, J = 7.4 Hz, 1H, H_{arom}), 7.11 (s, 1H, $CHCCH_2$), 3.54 (s, 2H, $CHCCH_2$), 0.25 (s, 9H, $Si(CH_3)_3$). ^{13}C-NMR (100 MHz, $CDCl_3$) δ 143.97, 142.95, 138.41, 127.28, 126.86, 126.00, 123.65, 121.61, 102.26, 99.47, 42.83, 0.16. HRMS (m/z) calcd for $C_{14}H_{17}Si$ [M + H$^+$] 213.10995, found 213.11035.

Synthesis of (C_9H_7)C≡CH (18). To a solution of **17** (2.53 g, 11.9 mmol, 1.0 eq.) in THF (30 mL) was added dropwise a solution of TBAF (14.4 mL, 1.0 M in THF, 14.4 mmol, 1.2 eq.) at 0 °C. The resulting purple solution was allowed to warm to room temperature and stirred at this temperature for 3.5 hours. ^{1}H NMR of the crude mixture showed that the reaction was done. The mixture was diluted with hexane (100 mL), washed with brine (30 mL × 1), dried over $MgSO_4$, filtered and evaporated *in vacuo*. The residue was purified by silica gel column (hexane) to give **18** (1.61 g, 96% yield) as a yellow liquid. ^{1}H-NMR (400 MHz, $CDCl_3$) δ 7.42 (d, J = 7.6 Hz, 1H, H_{arom}), 7.39 (d, J = 7.0 Hz, 1H, H_{arom}), 7.29 (t, J = 7.6 Hz, 1H, H_{arom}), 7.25 (dt, J = 7.4, 1.2 Hz, 1H, H_{arom}), 7.16 (s, 1H, $CHCCH_2$), 3.55 (s, 2H, $CHCCH_2$), 3.30 (s, 1H, C≡CH). ^{13}C-NMR (100 MHz, $CDCl_3$) δ 143.74, 142.92, 138.95, 126.92, 126.21, 126.15, 123.71, 121.70, 81.96, 81.04, 42.72. HRMS (m/z) calcd for $C_{11}H_9$ [M + H$^+$] 141.07043, found 141.07048.

Synthesis of (C_9H_7)CI=CH$_2$ (19). To a suspension of Ni(dppp)Cl_2 (58 mg, 0.1 mmol, 0.03 eq.) in THF (7 mL) was added dropwise a solution of DIBAL-H (7.2 mL, 1.0 M in hexane, 7.2 mmol, 2.0 eq.) at room temperature. The mixture was stirred for 5 minutes then it was cooled down to 10 °C. A solution of **18** (0.5 g, 3.57 mmol, 1.0 eq.) in THF (5 mL) was added and the resulting mixture was allowed to warm to room temperature and stirred at this temperature for 2 hours before a solution of iodine (2.7 g, 10.6 mmol, 3.0 eq.) in THF (20 mL) was added at 10 °C. The mixture was then stirred at room temperature for 40 minutes when TLC (hexane) showed the reaction was done. The mixture was diluted with diethyl ether (60 mL), washed with aqueous $Na_2S_2O_3$ (30 mL), dried over $MgSO_4$, filtered and evaporated at 30 °C *in vacuo*. The residue was purified by basic alumina column (0 → 3% EtOAc–hexane) to give **19** (0.6 g, 63% yield) as a yellow solid. ^{1}H-NMR (400 MHz, $CDCl_3$) δ 7.38 (dd, J = 6.4, 6.0 Hz, 2H, H_{arom}), 7.27 (t, J = 7.6 Hz, 1H, H_{arom}), 7.21 (dt, J = 7.4, 1.2 Hz, 1H, H_{arom}), 7.00 (s, 1H, $CHCCH_2$), 6.46 (d, J = 1.6 Hz, 1H, $CHHCI$), 5.97 (d, J = 1.6 Hz, 1H, $CHHCI$), 3.68 (s, 2H, $CHCCH_2$). ^{13}C-NMR (100 MHz, CD_2Cl_2) δ 147.62, 144.02, 143.87, 138.44, 127.15, 126.34, 124.33, 122.18, 102.55, 38.07. HRMS (m/z) calcd for $C_{11}H_{10}I$ [M + H$^+$] 268.98272, found 268.98267.

Synthesis of (C_9H_7)$_2$C=CH$_2$ (20). A Schlenk flask was charged with a magnetic stir bar and Mg turnings (0.32 g, 13.3 mmol, 3.0 eq.) and flame-dried under vacuum. After cooling, the flask was purged to N_2, anhydrous THF (6 mL) was added to just cover the turnings, and stirring was commenced. Several drops of 1,2-dibromoethane was added as initiator, and a heat gun used to briefly reflux the contents, after which the flask was placed in a 25 °C water bath. In a separate flame-dried flask under N_2 atmosphere, 2-bromoindene (0.87 g, 4.5 mmol, 1.0 eq.) was dissolved in THF (12 mL). A cannula was then used to transfer this solution onto the activated magnesium turnings over 5 min, resulting in a red, opaque solution. This solution was stirred at room temperature for 1.5 hours before it was added to a solution of $ZnCl_2$ (1.2 g, 8.8 mmol, 2.0 eq.) in THF (12 mL) in a flame-dried Schlenk flask at room temperature. The resulting mixture was cooled to 0 °C, and a solution of **4** (0.9 g, 3.4 mmol, 0.75 eq.) in THF (9 mL) and $Pd(PPh_3)_4$ (0.25 g, 0.2 mmol, 0.05 eq.) were added subsequently in turn. The resulting mixture was slightly evacuated and then filled with N_2 at 0 °C, and this process was repeated twice before it was stirred at this temperature for 1.5 hours. To the mixture was added ethyl acetate (50 mL) and water (20 mL), and the organic phase was separated. The aqueous layer was extracted with ethyl acetate (30 mL × 2) and the combined filtrates were washed with brine (20 mL × 1), dried over $MgSO_4$, filtered and evaporated *in vacuo*. The residue was purified by silica gel column (0 → 5% CH_2Cl_2–hexane, 0.1% Et_3N was added) to give **20** (0.4 g, 56% yield) as a yellow solid. ^{1}H-NMR (400 MHz, $CDCl_3$) δ 7.46 (d, J = 7.2 Hz, 2H, H_{arom}), 7.38 (d, J = 7.6 Hz, 2H, H_{arom}), 7.28 (t, J = 7.4 Hz, 2H, H_{arom}), 7.21 (dt, J = 7.4, 0.72 Hz, 2H, H_{arom}), 7.01 (s, 2H, C*H*CCH_2), 5.38 (s, 2H, $(C_9H_7)C{=}CH_2$), 3.71 (s, 4H, CHCCH_2). ^{13}C-NMR (100 MHz, $CDCl_3$) δ 146.60, 145.17, 142.90, 141.44, 130.41, 126.71, 125.15, 123.70, 121.30, 113.83, 40.43. HRMS (*m*/*z*) calcd for $C_{20}H_{17}$ [M + H$^+$] 257.13303, found 257.13289.

Synthesis of $(C_9H_7)_4C_4H_5$ (21). To a stirred solution of compound **20** (30 mg, 0.12 mmol, 1.0 eq.) and 1-hexene (0.15 mL, 1.2 mmol, 10.0 eq.) in CD_2Cl_2 (0.5 mL) was added a solution of Grubbs 2nd generation catalyst (5 mg, 0.006 mmol, 0.05 eq.) in CD_2Cl_2 (0.1 mL) at room temperature. The resulting brown solution was then stirred overnight and ^{1}H NMR showed the reaction was done. The mixture was concentrated and the residue was purified by silica gel column (0 → 3% EtOAc–hexane) to give compound **21** (25 mg, 81% yield) as a white solid. ^{1}H-NMR (400 MHz, $CDCl_3$) δ 7.47 (d, J = 7.36 Hz, 1H), 7.41 (d, J = 7.36 Hz, 1H), 7.38 (t, J = 7.48 Hz, 1H), 7.34 (d, J = 7.52 Hz, 1H), 7.10–7.26 (m, 9H), 7.02 (t, J = 7.4 Hz, 2H), 6.90 (d, J = 7.68 Hz, 1H), 6.82 (s, 1H), 6.52 (s, 1H), 6.43 (s, 1H), 4.66 (s, 1H), 4.07 (s, 2H), 3.73 (d, J = 22.4 Hz, 1H), 3.69 (s, 2H), 3.52 (d, J = 22.4 Hz, 1H), 3.09 (d, J = 23.2 Hz, 1H), 2.89 (d, J = 23.2 Hz, 1H), 2.45–2.79 (m, 4H). ^{13}C-NMR (100 MHz, $CDCl_3$) δ 156.83, 150.79, 147.80, 145.26, 145.09, 144.76, 143.88, 143.61, 143.55, 141.91, 138.63, 130.39, 129.69, 128.13, 127.29, 126.94, 126.83, 126.76, 126.39, 125.76, 125.23, 125.12, 124.60, 124.28, 124.07, 123.70, 123.61, 120.99, 120.95, 120.60, 56.03, 47.39, 41.53, 40.65, 39.30, 38.85, 37.51, 27.44. HRMS (*m*/*z*) calcd for $C_{40}H_{33}$ [M + H$^+$] 513.25823, found 513.25822.

Synthesis of $(H_2C{=}C(C_9H_6)_2)_2Zr$ (22). To a mixture of **20** (50 mg, 0.2 mmol, 1.0 eq.) and $NaN(SiMe_3)_2$ (79 mg, 0.43 mmol, 2.2 eq.) was added benzene (4 mL) at 25 °C. The resulting suspension was stirred at room temperature for overnight. To this yellow-orange suspension was added pyridine (50 μL, 0.62 mmol, 3.1 eq.) and $ZrCl_4(THF)_2$ (78 mg, 0.21 mmol, 1.05 eq.) in turn at room temperature. The mixture was stirred at room temperature for 3 hours before it was filtered through celite. The filtrate was concentrated *in vacuo*, washed by pentane, and dried under high vacuum to give **22** (43 mg, 74% yield) as a brown powder. Crystals suitable for X-ray diffraction were grown by vial-in-vial solvent diffusion of a concentrated solution of **22** in benzene with pentane. ^{1}H-NMR (400 MHz, C_6D_6) δ 6.87–6.97 (m, 16H, H_{arom}), 5.23 (s, 4H, $(C_9H_6)C{=}CH_2$), 5.19 (s, 8H, C*H*CC*H*). ^{13}C-NMR (100 MHz, C_6D_6) 141.90, 140.81, 134.75, 124.05, 123.13, 111.62, 103.22.

Synthesis of $H_2C{=}C(C_9H_6)_2ZrCl_2$ (23). To a stirred solution of **20** (0.26 g, 1.0 mmol, 1.0 eq.) in benzene (15 mL) was added $NaN(SiMe_3)_2$ (0.41 g, 2.2 mmol, 2.2 eq.) in one portion at 25 °C. The resulting yellow suspension was then stirred overnight. The suspension was filtered, and the residue was washed with benzene (5 mL) and pentane (10 mL), dried *in vacuo*. This yellow powder of di-sodium salt was added to a pre-cooled (−35 °C) suspension of $ZrCl_4(THF)_2$ (0.40 g, 1.05 mmol, 1.05 eq.) in toluene (10 mL) in portions, and the resulting suspension was allowed to warm to room temperature and stirred for 5 hours. The mixture was filtered through celite and the filter cake was washed with benzene (3 mL). The combined filtrates were concentrated *in vacuo*. Prior to the complete removal of solvent, excess hexane was added to precipitate the product, which was collected by filtration and dried under high vacuum to provide **23** (0.22 g, 52% yield) as a yellow powder. ^{1}H-NMR (400 MHz, C_6D_6) δ 7.43 (d, J = 3.08 Hz, 2H, H_{arom}), 7.41 (d, J = 3.08 Hz, 2H, H_{arom}), 6.96 (d, J = 3.04 Hz, 2H, H_{arom}), 6.94 (d, J = 3.08 Hz, 2H, H_{arom}), 5.52 (s, 4H, C*H*CC*H*), 5.29 (s, 2H, $(C_9H_6)C{=}CH_2$). ^{13}C-NMR (100 MHz, CD_2Cl_2) δ 138.12, 128.75, 126.82, 124.83, 117.77, 117.43, 101.76.

Synthesis of *n*-$C_4H_9CH{=}C(C_9H_6)_2ZrCl_2$ (24). To a stirred solution of compound **23** (30 mg, 0.072 mmol, 1.0 eq.) and 1-hexene (18 μL, 0.15 mmol, 2.0 eq.) in CH_2Cl_2 (2 mL) was added a solution of Grubbs 2nd catalyst (6.2 mg, 0.0073 mmol, 0.1 eq.) in CH_2Cl_2 (1 mL) at room temperature. The resulting brown solution was then stirred overnight before it was concentrated *in vacuo*. The residue was washed with pentane (2 mL), and then taken up in CH_2Cl_2 (1 mL). Excess hexane was added and the precipitate was discarded. The filtrate was then concentrated *in vacuo* to give compound **24** (9 mg, 28% yield) as a yellow-pink powder. ^{1}H-NMR (400 MHz, CD_2Cl_2) δ 7.54 (d, J = 3.2 Hz, 1H, H_{arom}), 7.53 (d, J = 3.2 Hz, 2H, H_{arom}), 7.51 (d, J = 3.2 Hz, 1H, H_{arom}), 7.26 (d, J = 3.2 Hz, 2H, H_{arom}), 7.25 (d, J = 3.2 Hz, 1H, H_{arom}), 7.24 (d, J = 3.2 Hz, 1H, H_{arom}), 6.21 (t, J = 8.0 Hz, 1H, C=C*H*CH_2), 6.03 (s, 2H, C*H*CCH), 6.01 (s, 2H, CHCC*H*), 2.40 (q, J = 8.0 Hz, 2H, C=CHCH_2), 1.58 (dd, J = 8.0 Hz, 2H, $CH_2CH_2CH_3$), 1.44 (m, 2H, $CH_2CH_2CH_3$), 0.96 (t, J = 7.6 Hz, 3H, $CH_2CH_2CH_3$). ^{13}C-NMR (100 MHz, C_6D_6) δ 133.60, 129.13, 128.88, 126.75, 126.66, 124.89, 117.76, 116.99, 102.64, 102.07, 31.75, 28.62, 22.51, 14.21.

Schlenk-flask polymerization experiments

These polymerizations were carried out using standard Schlenk-line techniques. A stock solution of 10 or 5 μmol pre-catalyst was prepared. In a Schlenk-flask, 1000 eq. MAO (10 wt% soln in PhMe) was syringed into anhydrous PhMe (50 mL PhMe was employed when 10 μmol pre-catalyst was used, and 200 mL PhMe for 5 μmol pre-catalyst) and attached to a line supplying 1 atm C_2H_4. Magnetic stirring was commenced at

1200 rpm. The flask was cycled between vacuum and ethylene (×3), then placed in a 25 °C water bath. The pre-catalyst was added *via* syringe; after 20 min, 10 mL of 10% (v/v) HCl in MeOH was used to carefully quench the reaction, a needle being used to vent the evolved gas. An additional 150 mL of MeOH was then added to fully precipitate any polymer. The resultant slurry was passed through filter paper and washed with further MeOH. The recovered polymer was dried in a vacuum oven at 60 °C overnight before it was weighed and analyzed. Condition A: the same procedure as before, except 100 eq. $i\text{-}Bu_3Al$ was used in place of MAO, and the pre-catalyst and $[Ph_3C][B(C_6F_5)_4]$ were combined briefly before syringing into the reaction flask. Copolymerizations with 1-hexene were performed in the same manner as in Condition A, except 5 mL 1-hexene was added 1 min. prior to addition of the pre-catalyst.

Autoclave polymerization experiments

Into 5 ml anhydrous toluene was suspended 1 mg of the appropriate complex **9a**, **10a**, **11a**, **9b**, **10b**, or (2-Ind)$_2$-1,1-biphenyl$ZrCl_2$. Methylaluminoxane (10 wt% soln in PhMe, M : Al = 1 : 1500) was added to the suspended complex (1.9 mL MAO solution for **9a**, 1.9 mL for **10a**, 2.18 mL for **11a**, 1.75 mL for **9b**, 2.08 mL for **10b** and 1.83 mL for (2-Ind)$_2$-1,1-biphenyl-$ZrCl_2$). After two minutes of shaking, the mixture was transferred under inert atmosphere into a 2 liter autoclave reactor maintained at 60 °C and filled with 250 mL of iso-pentane and 100 mL of 1-hexene. An ethylene pressure of 20 bar was applied for 1 hour. After releasing the pressure, the polymer was filtered through an airless filter funnel, washed with diluted hydrochloric acid (10 mL) water (10 mL) and acetone (10 mL) and finally dried in vacuum.

1-Hexene co-polymer quantification

^{13}C-NMR analysis was performed at 125 °C on a Varian 400 spectrometer. Samples were prepared in 10 mm tubes, 10 wt% polymer in 1,2,4-trichlorobenzene. A 5 mm sealed tube containing C_6D_5Br was inserted within the 10 mm NMR tube to serve as a deuterium lock. Parameter conditions for acquisition: 90° pulse angle, 33 s relaxation delay, 2 s acquisition time, and inverse gated ^1H decoupling. Signals were integrated and analyzed using the triad method developed by Hsieh and Randall.[21b]

X-ray crystallography

Crystals were coated in Paratone-N oil in the glovebox, mounted on a MiTegen Micromount and placed under an N_2 stream, thus maintaining a dry, O_2-free environment for each crystal. The data were collected on a Bruker Apex II diffractometer employing Mo Kα radiation (λ = 0.71073 Å). Data collection strategies were determined using Bruker Apex software and optimized to provide >99.5% complete data to a 2θ value of at least 55°. The data were collected at 150(±2) K for all crystals. The frames were integrated with the Bruker SAINT software package using a narrow-frame algorithm. Data were corrected for absorption effects using the empirical multi-scan method (SADABS). Non-hydrogen atomic scattering factors were taken from the literature tabulations.[34] The heavy atom positions were determined using direct methods employing the SHELXTL direct methods routine. The remaining non-hydrogen atoms were located from successive difference Fourier map calculations. The refinements were carried out by using full-matrix least squares techniques on F, minimizing the function $\omega(F_o - F_c)^2$ where the weight ω is defined as $4F_o^2/2s(F_o^2)$ and F_o and F_c are the observed and calculated structure factor amplitudes, respectively. In the final cycles of each refinement, all non-hydrogen atoms were assigned anisotropic temperature factors in the absence of disorder or insufficient data. In the latter cases atoms were treated isotropically. C–H atom positions were calculated and allowed to ride on the carbon to which they are bonded assuming a C–H bond length of 0.95 Å. H-atom temperature factors were fixed at 1.20 times the isotropic temperature factor of the C-atom to which they are bonded. The H-atom contributions were calculated, but not refined. The locations of the largest peaks in the final difference Fourier map calculation as well as the magnitude of the residual electron densities in each case were of no chemical significance.

Discussion

To synthesize the requisite ligands, 2-bromoindene (**1**)[25] was first transformed to the corresponding Grignard reagent, then transmetallated with tri-*n*-butyltin chloride to give the stannane $(2\text{-}C_9H_7)SnBu_3$ (**2**). Migita–Kosugi–Stille cross-couplings[35,36] with the *gem*-dibromides **3–5**,[26–28] were then accomplished under palladium-catalyzed conditions, providing the ligand precursors $R_2C{=}C(2\text{-}C_9H_7)_2$ (R = $C_{12}H_8$ **6**, Ph **7**, *n*-Pr **8**). It is noteworthy that attempts to use 1*H*-inden-2-ylboronic acid[37,38] or its trifluoroborate salt[39] for this later transformation gave very low yields.

The ligand dianions were most effectively generated by deprotonation with NaHMDS. Though subsequent salt metathesis with the simple $TiCl_3$, $TiCl_4$, or $ZrCl_4$ gave inconsistent results, reactions with $(Me_2N)_2TiCl_2$ and $(Me_2N)_2ZrCl_2\cdot DME$ cleanly yielded the desired *ansa*-metallocenes. Finally, treatment with trimethylsilyl chloride provided the dichlorides $R_2C{=}C(2\text{-}C_9H_7)_2MCl_2$ (R = $C_{12}H_8$, M = Ti: **9a**, Zr: **9b**; R = Ph, M = Ti: **10a**, Zr: **10b**; R = *n*-Pr, M = Ti: **11a**, Zr: **11b**) in yields ranging from 36–89% (Scheme 1).

All complexes were characterized by ^1H- and ^{13}C-NMR spectroscopy and elemental analysis. Indeed, the ^1H-NMR spectra of complexes **9–11** are informative in their characteristic indenyl singlets. The more electronegative titanium imparts further downfield chemical shifts than in the corresponding zirconium complexes. Moreover, it is clear that as the alkene substituent become more electron withdrawing (fluorenyl > diphenyl > di-*n*-propyl), the chemical shift of the indenyl singlet also moves further downfield, inferring that the alkene substituents are also playing an electronic role at the metal center.

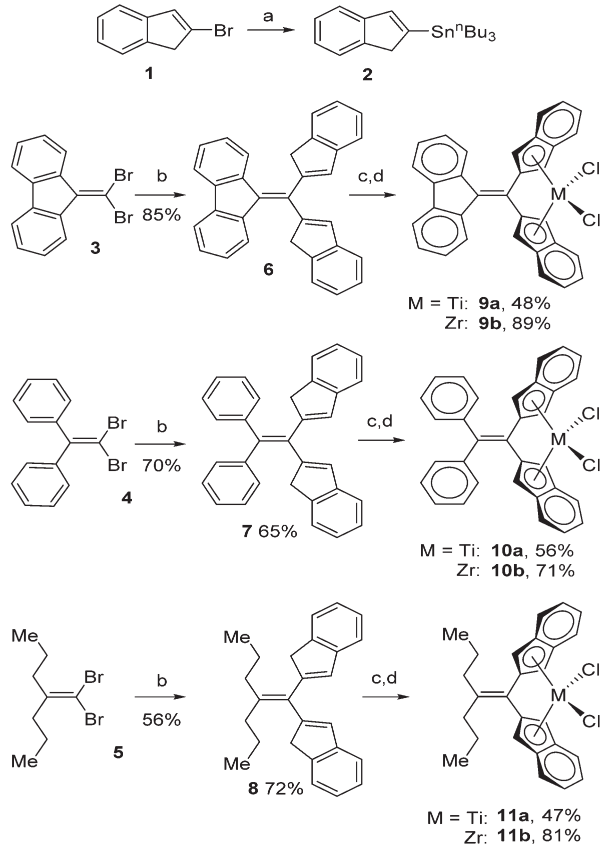

Scheme 1 Synthesis of metallocene complexes. Conditions: (a) Mg, cat. $BrCH_2CH_2Br$, THF, 25 °C, then *n*-Bu_3SnCl, THF, 0 °C; (b) 5 mol% $Pd_2(dba)_2$, 10 mol% *t*-Bu_3P, 2.5 eq. 2, PhMe; (c) 2.2 eq. $NaN(SiMe_3)_2$, THF, 0–25 °C, then $(Me_2N)_2ZrCl_2$·DME or $(Me_2N)_2TiCl_2$, 0–25 °C; (d) 3.0 eq. Me_3SiCl, CH_2Cl_2, 25 °C.

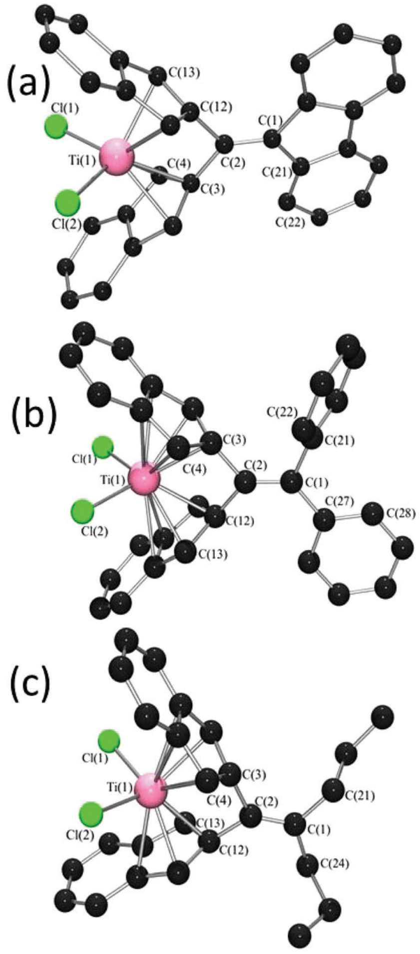

Fig. 2 POV-ray representation of complex (a) **9a**, (b) **10a**, (c) **11a**, C: black, Ti: violet, Cl: green. Hydrogens are omitted.

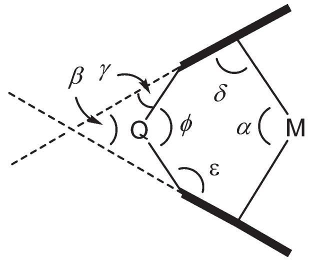

Fig. 3 Geometrical parameters for metallocene complexes.

Crystals suitable for X-ray diffraction were obtained for the three titanium complexes **9a**, **10a** and **11a** (Fig. 2), as well as for two of the zirconium complexes, **9b** and **10b**. In order to obtain quantifiable information on hapticity, differences in average metal to carbon bond lengths for the cyclopentadienyl-like ring portion of the indenyl systems were examined. The slip distortion parameter, (ΔM–C),[40] measures the average difference in distance between (a) the metal center and the two carbons shared by the 5- and 6-membered rings of the indenyl system and (b) the metal center and the three carbons unique to the 5-membered ring. Considering the two zirconium structures, the average (ΔM–C) value is calculated to be 0.160 Å for **9b** and 0.158 Å for **10b**. For comparison, the assumedly unstrained $(Ind)_2ZrCl_2$[41] and $(Ind)_2ZrMe_2$[42] have average (ΔM–C) values of 0.113 Å and 0.104 Å, respectively. Likewise, the titanium complex **9a** has an average (ΔM–C) value of 0.218 Å, **10a** of 0.202 Å, and **11a** of 0.195 Å; the related Ind_2TiMe_2[42] exhibits a value of 0.131 Å.

While these *ansa* species are then clearly more distorted than their parent unbridged structures, the slip parameters are small enough to place all complexes reported in this work within η^5 hapticity. Still, it is apparent that for the two metals studied, Zr exhibits a more natural fit into the ligand pocket, with Ti shifted further towards η^3 hapticity. Additionally, it appears that the alkene substituents play some role in the displacement of the metal, with (ΔM–C) growing larger with increasing electron-withdrawing effect. Finally, it is important to analyze the "openness" of the indene wedge. The most readily obtained value, Ct(1)–M–Ct(2) (*α*, Fig. 3), can be misleading, as a line connecting the metal to the indenyl centroid is not necessarily normal ($\delta \neq 90°$) to the plane of that ring. It is thus useful to consider the parameter *β*, the angle at which the indenyl planes would intersect were they to extend behind themselves into space.

Simple geometrical analysis reveals that $\beta = 360° - \alpha - \delta_1 - \delta_2$. Wang has compiled an excellent review of metrical parameters for a wide variety of *ansa*-metallocenes.[2] Overall, single sp^3 carbon bridges give values for β in the range of 65.6–66.9° for Ti and 69.5–72.8° for Zr metallocenes. Longer bridges, or single heteroatom linkages, invariably give smaller values. It is also worth noting the values of ϕ (see Fig. 3) obtained from these crystal structures. An sp^2-hybridized carbon is expected to exhibit unstrained bond angles of *ca.* 120°. Indeed, for the crystal structure of a ligand based on **6**, with triethylsilyl groups on the indenyl rings, a value of ϕ = 117.2° was observed.[43] In the complexes reported here, the bond angles at the bridging alkenyl carbon range between 101.3° and 104.5°. This angle compression presumably results from the η^5-hapticity of indenyl group at the metal. The most closely related complexes available in the literature are *ansa*-metallocenes based on 2,2′-methylenebis(1*H*-inden-1-yl)zirconium dichloride skeletons, three of which have been crystallographically analyzed.[44] For these sp^3-bridged structures, the largest value of ϕ obtained was 101.8°. In our series, the two comparable zirconium complexes **9b** and **10b** have ϕ = 104.5 and 103.8°, respectively, inferring the change from sp^3 to sp^2 hybridization at the bridge does enforce a more open indene–bridge–indene angle.

Values obtained for the present methylidene bridges (Table 1), particularly in the Ti series, are then touching at the upper limits of β. Surprisingly though, the aforementioned 2,2′-methylenebis(1*H*-inden-1-yl)zirconium dichloride systems,[44] while showing larger values for φ, maintain slightly smaller values for α (115.2–115.6°) and larger values for β (74.2–76.9°) compared to the zirconium complexes **10b** and **11b**. These methylene-bridged complexes, however, contain alkyl or silyl substituents on the indenyl rings, and hence steric repulsions may explain this observation.

Table 1 Selected bond lengths (Å) and angles (°)

	9a[a]	**10a**	**11a**	**9b**	**10b**
M–Cl(1)	2.301(9)	2.3101(6)	2.321(1)	2.407(2)	2.4219(6)
M–Cl(2)	2.302(5)	2.3219(6)	2.308(1)	—	2.4244(6)
M–C(3)	2.323(3)	2.342(2)	2.332(4)	2.451(6)	2.457(2)
M–C(4)	2.384(4)	2.355(2)	2.364(4)	2.480(5)	2.457(2)
M–C(5)	2.593(1)	2.539(2)	2.551(4)	2.626(5)	2.620(2)
M–C(10)	2.549(4)	2.563(2)	2.527(4)	—	2.640(2)
M–C(11)	2.339(3)	2.376(2)	2.343(4)	—	2.488(2)
M–C(12)	2.327(7)	2.343(2)	2.331(4)	2.448(6)[b]	2.467(2)
M–C(13)	2.342(4)	2.365(2)	2.371(4)	2.475(4)[c]	2.493(2)
M–C(14)	2.546(4)	2.567(2)	2.555(4)	2.621(4)[d]	2.633(2)
M–C(19)	2.588(1)	2.569(2)	2.537(4)	—	2.615(2)
M–C(20)	2.388(3)	2.365(2)	2.342(4)	—	2.455(2)
M–Ct(1)[e]	2.120	2.114	2.103	2.223	2.224
M–Ct(2)[e]	2.121	2.122	2.105	2.215	2.224
α	121.84	121.07	121.67	117.02	115.97
Cl(1)–M–Cl(2)	99.15(6)	98.49	100.24	103.95	100.09
C(1)–C(2)–C(3)	128.9(4)	126.26	129.07	126.94	128.01
C(1)–C(2)–C(12)	129.1(4)	132.39	128.62	128.55	128.16
ϕ	102.28	101.35	102.04	104.51	103.83
C(2)–C(1)–R(1)[f]	127.3(4)	116.27	120.33	128.26	121.11
C(2)–C(1)–R(2)[f]	127.28	125.20	121.61	126.63	121.74
R(1)–C(1)–R(2)	105.85	118.52	118.05	105.11	117.14
ε_1	164.20	163.79	163.03	163.14	164.41
ε_2	163.77	164.15	163.23	163.60	163.27
δ_1	83.71	84.94	85.10	85.81	85.98
δ_2	84.04	84.63	84.76	85.92	86.48
β	70.41	69.36	68.47	71.25	71.57
γ_1	15.80	16.21	16.97	16.86	15.59
γ_2	16.23	15.85	16.97	16.40	16.73

[a] Averaged. [b] M–C(8). [c] M–C(10). [d] M–C(11). [e] Ct(n) refer to the centroids of respective indenyl rings. [f] R(n) refer to the connecting non-indenyl carbons. ϕ: C(3)–C(2)–C(12); α: Ct(1)–M–Ct(2); ε_1: C(2)–C(3)–Ct(1); ε_2: C(2)–C(12)–Ct(2); δ_1: M–Ct(1)–C(3); δ_2: M–Ct(2)–C(12).

Further derivatization

Efforts to generate related alkylated ligands were undertaken. To this end, derivative **6** was sequentially reacted with two equivalents of NaN(SiMe$_3$)$_2$ at −35 °C and MeI affording the dimethylated ligand. Further treatment with LiN(SiMe$_3$)$_2$ and MeI afforded the tetramethylated ligand precursor (C$_{12}$H$_8$)C═C(C$_9$H$_5$Me$_2$)$_2$ (**12**) in 55% overall yield.

Initial efforts to metallate **12** involved reaction with NaN(SiMe$_3$)$_2$ and subsequent treatment with (Me$_2$N)$_2$TiCl$_2$. Isolation and characterization of the product **13** revealed the failure of this strategy to incorporate Ti. Instead the organic product (C$_{12}$H$_8$)C═C(C$_9$H$_4$Me$_2$)$_2$ **13** was isolated in 65% yield, in which the methylated indenyl rings are coupled (Scheme 2 and Fig. 4).

In contrast, reaction of **12** with two equivalents of NaN(SiMe$_3$)$_2$ and (Me$_2$N)$_2$ZrCl$_2$·DME afforded a new yellow species in 60% isolated yield. NMR data were consistent with the formulation of this species as (C$_{12}$H$_8$)C═C(C$_9$H$_4$Me$_2$)$_2$ZrCl$_2$ (**14**). This was subsequently confirmed by X-ray methods (Fig. 5). While the overall geometry of **14** is analogous to that of **9a** the impact of the methyl groups on the indenyl rings is to alter the ϕ angle to 106.7° with the average Zr–C distances to the η^3-bound indenyl rings of 2.46(3) Å and longer Zr–C distances of 2.501(8) and 2.61(1) Å.

An alternative strategy to derivatization of these metallocenes targeted the synthesis of a terminal methylene analog of **9–11**. The idea was to then employ this species as a synthon for olefin metathesis to access a family of ligands. To this end, an initial approach targeted a dehydration strategy to the olefinic ligand precursor. Thus, treatment of indenyl Grignard with acetyl chloride followed by an aqueous work-up was used to prepare (HO)CMe(C$_9$H$_7$)$_2$ (**15**), although it could only be isolated pure in 25% yield. Efforts to dehydrate **15** using *p*-tolylsulfonic acid as a catalyst resulted in dehydration and subsequent dimerization yielded C$_3$HMe(C$_9$H$_7$)$_4$ (**16**) in 50% yield (Scheme 3). The nature of this product was confirmed crystallographically (Fig. 6).

An alternative approach involved the high yielding synthesis of (C$_9$H$_7$)C≡CSiMe$_3$ (**17**) from 2-bromoindene, Me$_3$SiC≡CH and triethylamine using PdCl$_2$(PPh$_3$)$_2$/CuI as a catalyst. Subsequent conversion of **17** to **18** was achieved in 96% yield by treatment with [Bu$_4$N]F. Reductive iodination of the alkyne proceeded *via* treatment with Ni(dppp)Cl$_2$, DIBAL-H and iodine, affording (C$_9$H$_7$)CI═CH (**19**) in 63% yield (Scheme 4). Finally, reaction of **19** with the Mg, ZnCl$_2$ and Pd(PPh$_3$)$_4$ yielded

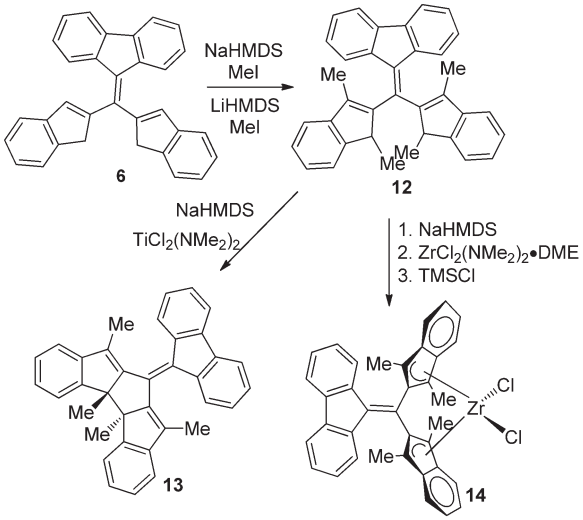

Scheme 2 Synthesis of **12–14**.

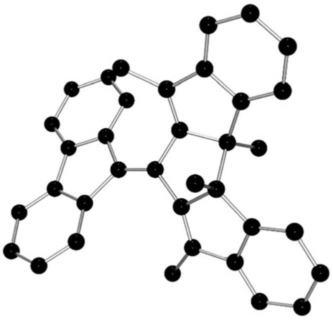

Fig. 4 POV-ray representation of complex **13**. Hydrogens are omitted.

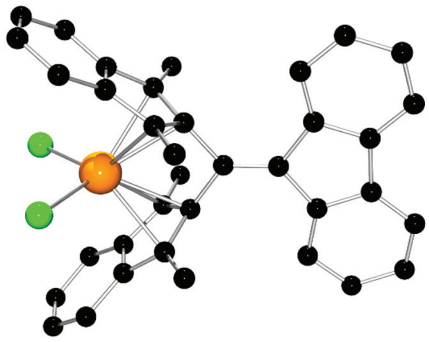

Fig. 5 POV-ray representation of complex **14**. C: black, Zr: coral, Cl: green. Hydrogens are omitted.

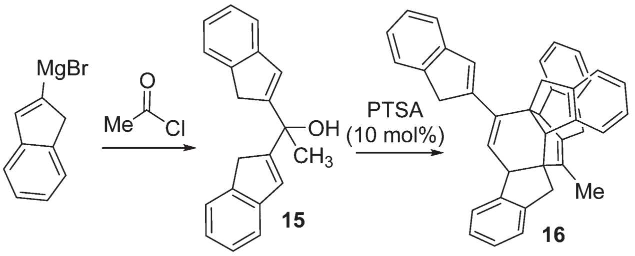

Scheme 3 Synthesis of **15–16**.

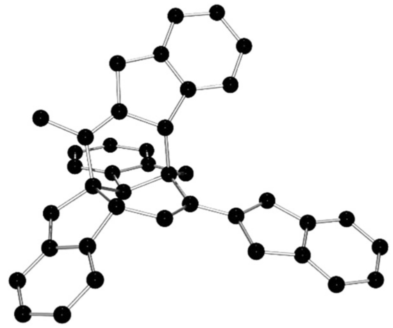

Fig. 6 POV-ray representation of complex **16**. Hydrogens are omitted.

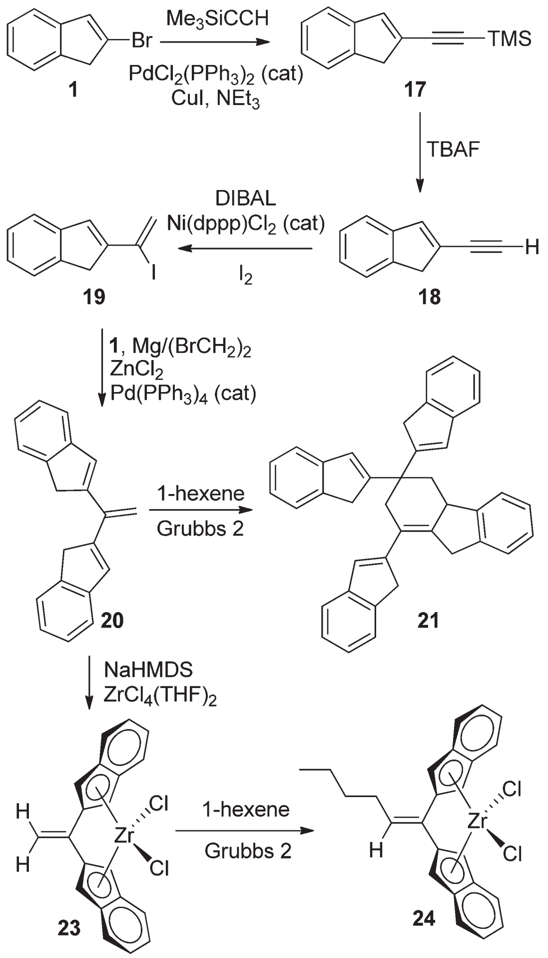

Scheme 4 Synthesis of **17–24**.

the desired 1,1-bis indenyl olefin, $(C_9H_7)_2C{=}CH_2$ (**20**), in 56% yield. Metathesis trials on **20** using Grubbs 2nd generation catalyst resulted in the formation of the cyclic dimeric species $(C_9H_7)_4C_4H_5$ (**21**) which was isolated in 81% yield as a white solid. Nonetheless, reaction of **20** with base and $ZrCl_4(THF)_2$ at room temperature led to the isolation of the bis-ligand

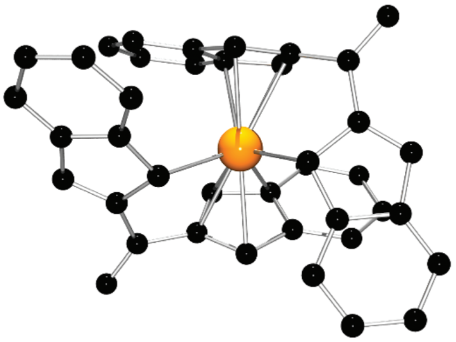

Fig. 7 POV-ray representation of complex **22**. Hydrogens are omitted.

complex, $(H_2C{=}C(C_9H_6)_2)_2Zr$ (**22**). The nature of **22** was confirmed crystallographically (Fig. 7). These data confirmed the formulation with two π-bound η^5-indenyl and two σ-bonded rings. The latter give rise to Zr–C bond distances of 2.342(3)Å. In contrast, performing the metallation procedures at −35 °C, the Zr complex, $H_2C{=}C(C_9H_6)_2ZrCl_2$ (**23**), was readily prepared. This afforded **23** in 52% yield as a yellow powder. Employing this species as a substrate for olefin metathesis with 1-hexene and again employing of Grubbs 2nd generation catalyst afforded the product n-$C_4H_9CH{=}C(C_9H_6)_2ZrCl_2$ (**24**) in 28% yield (Scheme 4).

Polymerization results

The synthesized complexes were tested for their ethylene polymerization activities in Schlenk-flask trials (Table 2) under atmospheric pressure conditions. Within a single metal series, yield of polymer from the two aryl-containing systems **9** and **10** are relatively similar; however, the alkyl systems **11** are markedly more active. Average molecular weights, moreover, do not appear to trend with the alkenyl substituents. Comparing the two metal systems, titanium consistently gave higher yields of polyethylene and with higher average molecular weights than zirconium.

As the metal center is comparatively exposed in these systems, this could lead to chain transfer to the methylaluminoxane (MAO) co-catalyst, particularly with the zirconium precatalysts. Consequently, **11a** and **11b** were run using i-Bu_3Al as alkylating agent/solvent scrubber and $[Ph_3C][B(C_6F_5)_4]$ as initiator.[45,46] While this did increase the average molecular weights of the resulting polymer, it came at the expense of lower overall activities.

The metallocenes **9–11** were also tested in 1-hexene–ethylene co-polymerization experiments utilizing both Schlenk-line and autoclave vessels (Tables 3 and 4, respectively). For comparative purposes, the known bis(1*H*-inden-2-yl)-1,1′-biphenylzirconium dichloride[47] was also tested under identical conditions, as the biphenyl moiety of this complex was expected to provide a similar inductive effect as the aryl groups in complexes **9b** and **10b**. However, the difference in geometry (α = 132°) putatively provides a less open metallocene.

While activity measurements between Tables 3 and 4 cannot be directly compared, it is evident that the increased quantity of polymer produced occurs as a result of 1-hexene

Table 2 Ethylene polymerizations[a]

Precat. (μmol)	MAO (mmol)	Vol (mL)	Yield (g)	Act. (g mmol^{-1} h^{-1})	M_w (Da)	PDI
9a (10)	10	50	1.86	560	122 000	3.6
10a (10)	10	50	1.60	480	154 000	3.8
11a (5)	10	200	4.10	2460	137 000	3.3
11a (10)	A	50	1.68	500	145 000	3.3
9b (10)	10	50	1.51	450	2500	2.0
10b (10)	10	50	1.16	350	2800	1.8
11b (10)	10	200	2.06	1240	2500	1.8
11b (10)	A	50	1.51	450	4900	2.5

[a] Conditions: 1 atm C_2H_4; 25 °C, 20 min PhMe. A: 1 mmol iBu_3Al, 11 μmol $[Ph_3C][B(C_6F_5)_4]$.

Table 3 Ethylene–1-hexene copolymerization (low pressure)

Precat.	Yield (g)	Act. (g mmol^{-1} h^{-1})	Hexene incorp. (mol %)
9a	5.42	1620	17.2
10a	5.09	1530	15.2
11a	6.50	1950	8.4
9b	3.94	1180	28.2
10b	3.72	1120	28.4
11b	6.58	1970	16.8
$BIBPZrCl_2$[a]	1.53	461	6.6

Conditions: 10 μmol precat., 10 mmol MAO, 1 atm C_2H_4, 5 mL 1-hexene, 50 mL PhMe, 25 °C, 20 min. Hexene incorporation determined by ^{13}C-NMR analysis. [a] $BIBPZrCl_2$ = (2-Ind)$_2$-1,1-biphenyl$ZrCl_2$.

Table 4 Ethylene–1-hexene copolymerization, autoclave experiments

Precat.	Productivity (g_{copol}/g_{precat})	Branching[a]	Density (g mL^{-1})	M_w (Da)	PDI	T_c (°C)	T_m (°C)
9a	103 000	13.67	0.9392	292 500	3.1	113	127
10a	28 000	17.68	0.9317	313 000	2.9	115	129
11a	96 000	20.51	0.9246	122 500	2.2	110	122
9b	19 000	117.02	0.9330	2700	1.8	98	106
10b	27 000	115.97	0.9345	3100	1.9	100	109
$BIBPZrCl_2$[b]	79 000	16.34	0.9398	381 000	2.3	117	131

Conditions: 1 mg precat., MAO (M : Al ratio 1 : 1500), 20 bar C_2H_4, 100 mL 1-hexene, 250 mL iso-pentane, 60 °C, 1 h. [a] Per 1000 carbon atoms. [b] $BIBPZrCl_2$ = (2-Ind)$_2$-1,1-biphenyl$ZrCl_2$.

incorporation. Across Tables 3 and 4, the Zr systems appear to give greater 1-hexene incorporation than the Ti complexes. However, the very low molecular weights of the resultant polymers probably causes an inflation in this value: the ^{13}C-NMR analysis assumes a low concentration of end groups, which give signals overlapping with the 1-butene side chains of the copolymer.

Conclusion

This study has detailed the synthesis of a new class of titanium and zirconium *ansa* metallocene complexes. The large deviations from ideal sp^2-hybridized carbon bond angles in the ligands leads us to believe that these complexes push at the geometrical limits for such structures, and hence at how open a metallocene wedge can be made. In polymerization experiments, the zirconium complexes are active in the production of very low molecular weight polyethylene, while the analogous titanium complexes provide overall good activities for higher molecular weight polymer. Finally, the open metal sites of the synthesized complexes allow for the uptake of 1-hexene in copolymerization experiments.

Metrical parameters appear to vary only slightly with the nature of the alkene substituents and without a clear pattern. However, polymerization activities show a more distinct trend, with an electron releasing group enhancing activity and electron withdrawing groups increasing co-monomer incorporation. Further derivatization of the alkenes, particularly by substituting the aryl rings of ligand **7** may provide both better understanding and fine tuning of the catalyst behaviour and polymer properties. Such efforts are continuing.

Notes and references

1 M. P. McDaniel, *Handbook of Transition Metal Polymerization Catalysts*, Wiley, New Jersey, 2010.

2 B. Wang, *Coord. Chem. Rev.*, 2006, **250**, 242–258.

3 S. Prashar, A. Antinolo and A. Otero, *Coord. Chem. Rev.*, 2006, **250**, 133–154.

4 C. L. Lund, S. S. Hanson, G. Chatte, J. W. Quail and J. Müller, *Organometallics*, 2010, **29**, 6038–6044.

5 D. Kazul'kin, A. N. Ryabov, V. V. Izmer, A. V. Churakov, I. P. Beletskaya, C. J. Burns and A. Z. Voskoboynikov, *Organometallics*, 2005, **24**, 3024–3035.

6 D. S. Stelck, P. J. Shapiro, N. Basickes and A. L. Rheingold, *Organometallics*, 1997, **16**, 4546–4550.

7 C. Takayama, Y. Yamaguchi, T. Mise and N. Suzuki, *J. Chem. Soc., Dalton Trans.*, 2001, 948–953.

8 D. W. Stephan, *Organometallics*, 2005, **24**, 2548.

9 A. L. McKnight and R. M. Waymouth, *Chem. Rev.*, 1998, **98**, 2587–2598.

10 T. Matsugi and T. Fujita, *Chem. Soc. Rev.*, 2008, **37**, 1264–1277.

11 D. Takeuchi, *Dalton Trans.*, 2010, **39**, 311–328.

12 V. C. Gibson and S. K. Spitzmesser, *Chem. Rev.*, 2003, **103**, 283–315.

13 G. J. P. Britovsek, V. C. Gibson and D. F. Wass, *Angew. Chem., Int. Ed.*, 1999, **38**, 428–447.

14 J. W. Lauher and R. Hoffman, *J. Am. Chem. Soc.*, 1976, **98**, 1729–1742.

15 P. Margl, L. Deng and T. Ziegler, *Organometallics*, 1998, 17.

16 P. Margl, L. Deng and T. Ziegler, *J. Am. Chem. Soc.*, 1998, 120.

17 P. Margl, L. Deng and T. Ziegler, *J. Am. Chem. Soc.*, 1999, 121.

18 H. Alt and A. Köppl, *Chem. Rev.*, 2000, 100.

19 J. Martinez-Salazar, *Organometallics*, 2014, **33**, 2944–2959.

20 C. E. D. Zachmanoglou, A. Bridgewater, B. M. Parkin, G. Brandow, C. G. Bercaw, J. E. Jardine, C. N. Lyall, M. Green, J. C. Keister and J. B. Keister, *J. Am. Chem. Soc.*, 2002, **124**, 9525–9546.

21 (*a*) D. J. Arriola, E. M. Carnahan, P. D. Hustad, R. L. Kuhlman and T. T. Wenzel, *Science*, 2006, 312; (*b*) E. T. Hsieh and J. C. Randall, *Macromolecules*, 1982, **15**, 1402.

22 G. W. H. Coates, P. D. Hustad and S. Reinartz, *Angew. Chem. Int. Ed.*, 2002, **41**, 2236–2257.

23 W. Kaminsky, *Macromol. Chem. Phys.*, 1996, **197**, 3907–3945.

24 2007.

25 I. Mc Ewen, M. Roennqvist and P. Ahlberg, *J. Am. Chem. Soc.*, 1993, **115**, 3989–3996.

26 G. C. Paul and J. J. Gajewski, *Synthesis*, 1997, 524–526.

27 P. M. Donovan and L. T. Scott, *J. Am. Chem. Soc.*, 2004, **126**, 3108–3112.

28 H. Rezaei and J. F. Normant, *Synthesis*, 2000, 109–112.

29 T. H. Warren, G. Erker, R. Fröhlich and B. Wibbeling, *Organometallics*, 2000, **19**, 127–134.

30 E. Benzing and W. Kornicker, *Chem. Ber.*, 1961, **94**, 2263–2267.

31 C. Wang, G. Erker, G. Kehr, K. Wedeking and R. Fröhlich, *Organometallics*, 2005, **24**, 4760–4773.

32 A. B. Pangborn, M. A. Giardello, R. H. Grubbs, R. K. Rosen and F. J. Timmers, *Organometallics*, 1996, **15**, 1518–1520.

33 W. C. Still, M. Kahn and A. Mitra, *J. Org. Chem.*, 1978, **43**, 2923–2925.

34 D. T. Cromer and J. T. Waber, *Int. Tables X-Ray Crystallogr.*, 1974, **4**, 71–147.

35 W. Shen and L. Wang, *J. Am. Chem. Soc.*, 1999, **64**, 8873–8879.

36 L. Kurti and B. Czako, *Strategic Applications of Named Reactions in Organic Synthesis*, Elsevier, Massachusetts, 2005.

37 E. G. IJpeij, F. H. Beijer, H. J. Arts, C. Newton, J. G. de Vries and G.-J. M. Gruter, *J. Org. Chem.*, 2002, **67**, 169–176.

38 A. Bauer, M. W. Miller, S. F. Vice and S. W. McCombie, *Synlett*, 1995, 254–256.

39 E. Vedejs, R. W. Chapman, S. C. Fields, S. Lin and M. R. Schrimpf, *J. Org. Chem.*, 1995, **60**, 3020–3027.

40 J. W. Faller, R. H. Crabtree and A. Habib, *Organometallics*, 1985, **4**, 929–935.

41 T. Repo, M. Klinga, I. Mutikainen, Y. Su, M. Keskelä and M. Polamo, *Acta Chem. Scand.*, 1996, **50**, 1116–1120.

42 J. L. Atwood, W. E. Hunter, D. C. Hrncir, E. Samuel, H. Alt and M. D. Rausch, *Inorg. Chem.*, 1975, **14**, 1757–1762.

43 Formula: $C_{44}H_{50}Si_2$; 635.02 g mol^{-1}; triclinic, $P\bar{1}$; a = 8.397(1), b = 12.138(1), c = 18.422(2) Å; α = 103.273(6), β = 93.615(7), γ = 92.848(6)°; Z = 2; d_{calc} = 1.159 g cm^{-3}; abs. coeff. 0.127 mm^{-1}, refl. collected: 42 063, unique: 11 574; R_1 = 0.0455; wR_2 = 0.1347.

44 L. Resconi, I. Camurati, C. Fiori, D. Balboni, P. Mercandelli and A. Sironi, *Helv. Chim. Acta*, 2006, **89**, 1497–1523.

45 I. Kim and R. F. Jordan, *Macromolecules*, 1996, **29**, 489–491.

46 N. N. Bhriain, H.-H. Britzinger, D. Ruchatz and G. Fink, *Macromolecules*, 2005, **38**, 2056–2063.

47 W. W. Ellis, T. K. Hollis, W. Odenkirk, J. Whelan, R. Ostrander, A. L. Rheingold and B. Bosnich, *Organometallics*, 1993, **12**, 4391–4401.